

# Imprint of Early Dark Energy in Stochastic Gravitational Wave Background

Chia-Feng Chang<sup>1,\*</sup>

<sup>1</sup>*Department of Physics and Astronomy, University of California, Riverside, CA 92521, USA*  
(Dated: March 29, 2022)

Early dark energy that relieves Hubble tension leaves a fingerprint in the primordial stochastic gravitational wave background that originates from cosmic string network. We show that the signal is not only detectable with future planned gravitational wave experiments, but also distinguishable from other astrophysical and cosmological signals in the gravitational wave frequency spectrum.

## INTRODUCTION

Gravitational waves (GWs) search technologies [1–5] have strong ongoing research interest. Implications from these developments focus not only on discovering new astrophysical objects [6, 7], but also probing gravitation physics [8–13] and non-standard cosmologies [14–21]; and GW observations has been used to measure the current Hubble rate  $H_0$  [22–25]. Although not yet sufficiently precise to resolve the Hubble tension, estimates will be continuously improved.

Increasingly attention is focusing on possible solutions of Hubble tension, a Hubble rate discrepancy between local observations, such as supernovae signals [26–31], lensing time delays [32–38] and non-local searches, e.g. the cosmic microwave background (CMB) [39–42]. Local measurements confirm  $H_0$  is approximately five sigma statistical significance above observation in the CMB with assuming standard cosmological model ( $\Lambda$ CDM). This strong disagreement has been closely examined using many statistical [43–46] and measurement methods [31, 36, 47–50], and re-examining potential technical issues [51–56] in both local and CMB measurements (see reviews [48, 57–59]). Various evidence suggests the discrepancy arises due to a currently unknown physical phenomenon outside conventional  $\Lambda$ CDM predictions.

V. Poulin *et al.* [60–62] showed that early dark energy (EDE) behaves as a cosmological constant when comoving scaling factor  $a(t)$  is smaller than critical  $a_c \sim 10^{-4}$ , and is then diluted faster or equal to radiation-like component to relieve the Hubble tension. EDE contributes up to 20% energy density of the universe (model-dependent) at  $a_c$ , consequently accelerating the universe expansion and hence slightly delaying the universe entering the matter-domination era. This framework brings  $H_0$  in estimated CMB to be consistent with local measurements and also with measured high and low redshifts [63–66].

We adopted the simplest EDE model, i.e., slow-rolling potential  $V(\phi) \propto \phi^{2n}$  with scalar field  $\phi$  [67–69]. Effective mass for  $\phi$  is lighter than the Hubble rate on the early universe, and hence Hubble friction overdamps scalar field motion and freezes it. Consequently, the scalar field behaves as a subdominant cosmological constant until the Hubble rate decreases to approximately scalar effec-

tive mass, namely, the driving force overcomes the Hubble friction. Subsequently, the field starts oscillating as a fluid with equation of state  $w_\phi = (n-1)/(n+1)$ .

Cosmic strings, one dimension long-lived topological defects, are stable and predictable sources for stochastic GW background (SGWB) and hence ideal creator sources for GW as a messenger that carries new signal from the early universe [70–72]. Such stable objects arise from beyond standard model theories, such as spontaneously broken  $U(1)$  [73–76] or superstring theories [77–80]. The GW frequency spectrum formed by the cosmic string network is an approximate plateau over a broad frequency range with parameter  $G\mu$  dependence, where  $G$  is the Newtonian gravitational constant and  $\mu$  is string tension. GW experiments EPTA [81] and PPTA [82] provide strong bounds on  $G\mu \lesssim 2 \times 10^{-11}$  [17], but this remains in tension with the NANOGrav 12.5yr result [83]  $G\mu \in (2, 30) \times 10^{-11}$  in 95% C.L. [84, 85]. The tension may be due to the different noise analysis methods [86].

This paper shows that EDE imprints a GW signal in the SGWB formed from the cosmic string network that is distinguishable from other astrophysical and cosmological signals in the GW frequency spectrum. Such a unique spectrum could be detected in future GW experiments LISA [87–89] and SKA [90]. We also contour the SKA and LISA sensitivities on EDE parameter space.

## FRAMEWORK

Nambu-Goto string action is an effective model that describes cosmic string network evolution [91]. These strings formed at time  $t_F$  when temperature cools to symmetry breaking scale of theory. Shortly after, the defects behave as a scaling invariant network that includes a few long (super-horizon length) strings and a collection of closed loops chopped from long strings. GW loop emission dominates the network energy loss, and loop number density  $n_o(t_i, t)$  is characterized by [76]

$$dn_o(t_i, t) = \frac{0.1}{\alpha} \int_{t_F}^t C_{\text{eff}}(t_i) \frac{dt_i}{t_i^4} \left( \frac{a(t_i)}{a(t)} \right)^3, \quad (1)$$

where loops form at  $t_i$  and subsequently continuously diluted until time  $t$ , factor 0.1 represents 90% string energy release to loop kinetic energy and subsequent diluted off,

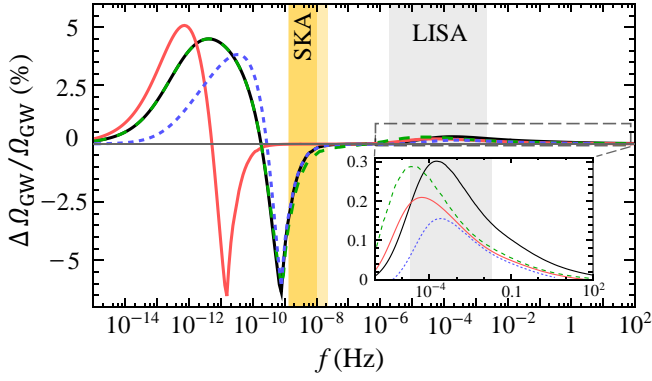


FIG. 1: Signal difference ratio versus GW frequencies as defined in Eq.(6). The black solid curve:  $G\mu = 10^{-12}$ ,  $a_c = 10^{-4.48}$ ,  $n = 2$  and  $f_{\text{EDE}} = 4\%$ . According to black curve, others are changing one parameter on each, e.g. red: change  $a_c \rightarrow 10^{-3.57}$ , green:  $G\mu \rightarrow 10^{-11}$ , and blue:  $n \rightarrow 3$ . The  $a_c$  correspond to highest and lowest values in 68%C.L. CMB analysis [60]. LISA and SKA sensitivities targeting  $G\mu = 10^{-12}$  cosmic string GW spectrum (see Fig. 2 in [17]) show as gray and yellow area, respectively. The lighter yellow is for  $G\mu = 10^{-11}$ .

and parameter  $\alpha = 0.1$  [92, 93] characterize initial loop size  $\ell(t_i) = \alpha t_i$ . The appendix reviews the simulation calibration parameter  $C_{\text{eff}}$  [17, 18], which controls loop production. Created loops are shortened by radiating GWs

$$\ell(t) = \alpha t_i - \Gamma G\mu(t - t_i), \quad \text{with } t \geq t_i, \quad (2)$$

where GW emission parameter  $\Gamma = 50$  [92–96]. Loop emission characterizes in normal modes  $k \in \mathbb{Z}^+$  oscillation with emitted GW frequency,

$$f = \frac{2k}{\ell} = \frac{a(t)}{a(t_0)} \frac{2k}{\alpha t_i - \Gamma G\mu(t - t_i)}, \quad (3)$$

where emitted GWs redshift to today ( $t_0$ ).

Thus, the SGWB frequency spectrum can be computed by summing all normal modes,

$$\Omega_{\text{GW}}(f) = \frac{f}{\rho_c} \frac{d\rho_{\text{GW}}}{df} = \sum_k \Omega_{\text{GW}}^{(k)}(f), \quad (4)$$

with

$$\begin{aligned} \Omega_{\text{GW}}^{(k)}(f) &= \frac{1}{\rho_c} \frac{2k}{f} \frac{F_\alpha \Gamma^{(k)} G\mu^2}{\alpha(\alpha + \Gamma G\mu)} \\ &\times \int_{t_F}^{t_0} dt \frac{C_{\text{eff}}(t_i)}{t_i^4} \left(\frac{a(t)}{a(t_0)}\right)^5 \left(\frac{a(t_i)}{a(t)}\right)^3 \theta(t_i - t_F) \theta(\ell(t)), \end{aligned} \quad (5)$$

where critical density  $\rho_c = 3H_0^2/8\pi G$ , cusp dominates GW emission  $\Gamma^{(k)} = \Gamma/(3.6 k^{4/3})$  [17], and we sum over  $k$  modes up to  $k \leq 10^5$ .

To visualize EDE influence on SGWB, we define signal difference to SGWB spectrum ratio as,

$$\frac{\Delta\Omega_{\text{GW}}}{\Omega_{\text{GW}}}(f) \equiv \frac{\Delta\Omega_{\text{GW}}(f)}{\Omega_{\text{GW}}^{\text{ACDM}}(f)} \equiv \frac{\Omega_{\text{GW}}^{\text{EDE}}(f) - \Omega_{\text{GW}}^{\text{ACDM}}(f)}{\Omega_{\text{GW}}^{\text{ACDM}}(f)}, \quad (6)$$

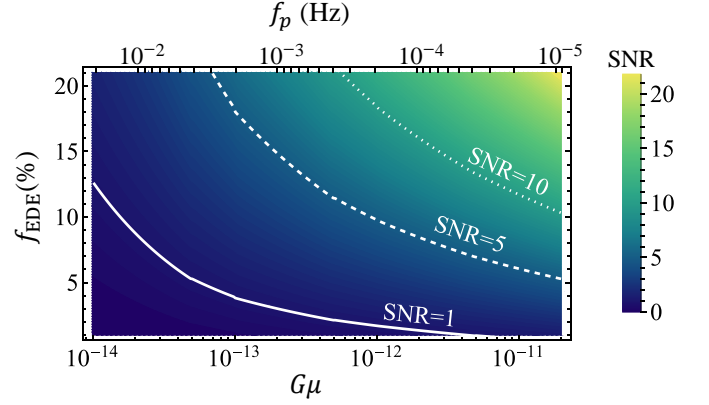


FIG. 2: Energy density fraction of early dark energy  $f_{\text{EDE}}$  versus string tension parameter  $G\mu$  with peak frequency  $f_p$  on upper  $x$ -axis, and fixing early dark energy potential exponent parameter  $n = 2$  and critical redshift  $a_c = 10^{-4.48}$ . The colored region shows influenced cosmic string GW background Signal-to-Noise Ratio (SNR) with LISA 4 years nominal mission operating period, see Eq.(10).

where superscripts imply GW frequency spectra on different cosmologies. Fig. 1 shows that EDE modifies the spectrum in two frequency regions: firstly, in contrast to  $\Lambda$ CDM, diluting EDE delays entering of matter domination, which slows down the redshift on GWs that emitted by the loops with loop formation time  $t_i \lesssim \Gamma G\mu t_c/\alpha$  where  $t_c$  is the universe age at  $a_c$ . This mechanism *peaks* the GW spectrum at frequency  $f \sim 10^{-4}$  Hz. The resulting spectrum typically increases at characterized frequency  $f_p$ , which can be estimated from Eq.(3) as,

$$f_p \sim \frac{2\epsilon}{\Gamma G\mu t_c} \frac{a_c}{a(t_0)}, \quad (7)$$

where  $\epsilon \sim \mathcal{O}(1)$  is a numerical parameter. The shape of this peak approximately estimate to

$$\frac{\Delta\Omega_{\text{GW}}}{\Omega_{\text{GW}}}(f) \propto \begin{cases} \left(\frac{f}{f_p}\right)^{-0.23}, & \text{for } f \geq f_p, \\ \left(\frac{f}{f_p}\right)^3, & \text{for } f < f_p, \end{cases} \quad (8)$$

and the slower diluting EDE (lower  $n$ ) more significantly delays the universe entering the matter domination epoch while GWs experience a longer and slower dilution period, hence increasing the signal difference.

Second, faster universe expansion at  $t_c$  reduces loop chopping efficiency i.e., reduces  $C_{\text{eff}}(t_i = t_c)$  in Eq.(1), due to less frequent intercommutation between strings. Such a mechanism implies a signal difference *dip* at characteristic frequency  $f_d \sim 10^{-9}$  to  $10^{-11}$  Hz as shown in Fig. 1, which can be computed from Eq.(3) with GWs emission today,

$$f_d \sim \frac{2}{\alpha t_c}. \quad (9)$$

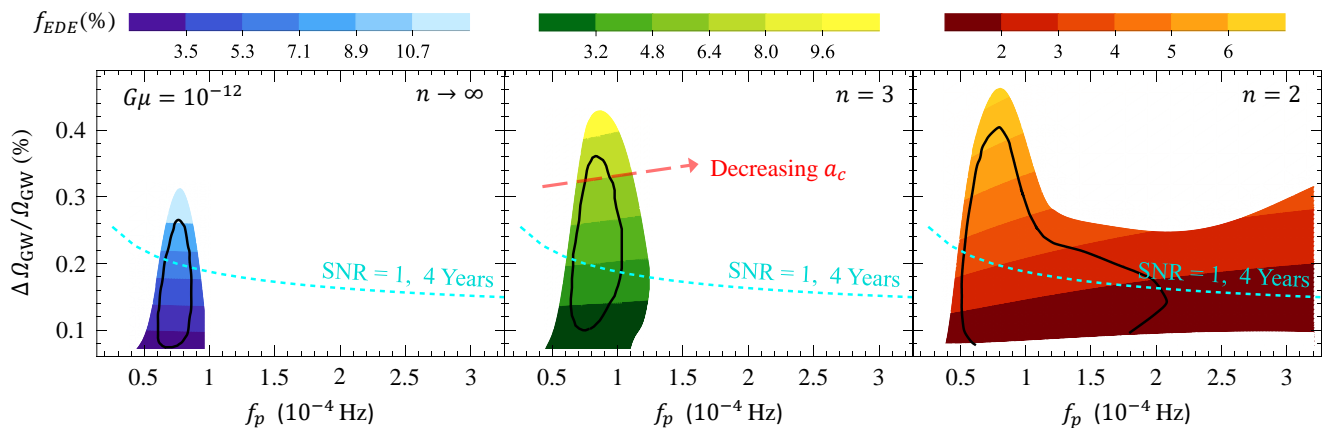


FIG. 3: GW spectrum difference ratio  $\Delta\Omega_{\text{GW}}/\Omega_{\text{GW}}$  at peak frequency  $f_p$  with fixed  $G\mu = 10^{-12}$ . The colored areas and the black circled areas represent the 95% C.L. and 68% C.L. in CMB numerical analysis, respectively. The CMB analysis is directly quoted from [60], they scan early dark energy (EDE) total energy fraction  $1\% \leq f_{\text{EDE}} \leq 13\%$  and critical scaling factor  $10^{-4.8} \leq a_c \leq 10^{-3.4}$  in different EDE potential  $\phi^{2n}$  exponents  $n = \{2, 3, \infty\}$ . The dashed curves show the signal-noise-ratio SNR = 1 with LISA 4 years collection. The curves on the boundaries between each color (e.g. between lighter green and green) are  $a_c$  variations with fixed  $f_{\text{EDE}}$  as the red dashed line.

Shortly after  $t_c$ , more long strings have entered the horizon, loop chopping efficiency turns back to about that for  $\Lambda\text{CDM}$ , and again, the delayed entering of matter domination era. Therefore, loop number density increases slightly, and redshift effects on GW slow. This mechanism increases signal difference at frequencies below but close to  $f_d$ .

Universal fitting on a wide frequency spectrum not only determines string tension parameter  $G\mu$ , but also addresses EDE parameters.  $f_{\text{EDE}}$  proportionally controls both signal difference peak and dip amplitudes, whereas peak amplitude is sensitive to  $n$  but dip amplitude is independent. Therefore, we expect peak and dip amplitudes pin down  $f_{\text{EDE}}$  and  $n$ , and  $f_d$  and  $f_p$  can be used to address  $a_c$  (as shown in Fig. 1).

Modified GW frequency spectra present in LISA [87–89] and SKA [90] frequency sensitivities (Fig. 1) and hence we focus on analyzing signal-to-noise ratio (SNR) for the remainder of this paper.

## SIGNAL-TO-NOISE RATIO

Early dark energy has relatively small energy contribution in the early universe, hence its influence GW variation is small compared to string SGWB, but could still be larger than noise background if string tension is sufficiently large. For comparing signal difference and noise background, we define SNR as  $\{i = \text{SKA}, \text{LISA}\}$

$$\text{SNR} = \sqrt{T_i \int_{f_{\min}}^{f_{\max}} df \left( \frac{\Delta\Omega_{\text{GW}}(f)}{\Omega_n^i(f)} \right)^2}, \quad (10)$$

where the SKA and LISA are calculated separately, frequency is integrated on the experimental sensitivity re-

gion,  $T_i$  is the observation period, and  $\Omega_n^i(f)$  is an effective strain noise spectral spectrum for LISA and SKA, respectively. SNR analysis has been widely studied [97–100] and numerical details are provided in the appendix.

The peak frequency  $f_p$  is within the LISA goal sensitivities  $20\mu\text{Hz} \leq f \leq 1\text{Hz}$  [87] for  $G\mu \leq 2 \times 10^{-11}$  as presented in Fig. 2, and the peaky signal is more significant than noise background for most of interesting parameter space. More string energy causes stronger cosmic string SGWB, and hence the signal is more significant for larger  $G\mu$ .

Fig. 3 shows signal difference ratio  $\Delta\Omega_{\text{GW}}/\Omega_{\text{GW}}$  at peak frequency  $f_p$ . The colored areas were studied in CMB analysis [60] for relieving the Hubble tension. We explicitly show that the signal difference could exceed the noise background (SNR > 1) in the 4 years LISA collection, and therefore the EDE signal is detectable. As discussed, lower  $n$  has a larger signal difference due to the later universe transition to matter-domination era.

Fig. 4 shows LISA and SKA detection sensitivities to EDE parameter space. Signal difference can be larger than noise background over few frequency decades, including most sensitive LISA regions, see the gentle slope  $f^{-0.23}$  over frequencies  $f > f_p$  in Eq.(8). Thus, LISA can capture the EDE signal even though  $f_p$  is outside LISA sensitivities. Higher  $a_c$  corresponds to lower SNR because  $f_p$  moves away from LISA sensitivities with increasing  $a_c$ .

The pulsar timing detector SKA can capture (SNR > 1) the signal difference dip, as presented in Fig. 4. There are two falls on the SKA curves on the left-panel: the fall on lower  $a_c$  is caused by the dip in signal difference; whereas the fall on higher  $a_c$  is due to the signal difference peak. If the NANOGrav signal is due to cosmic string

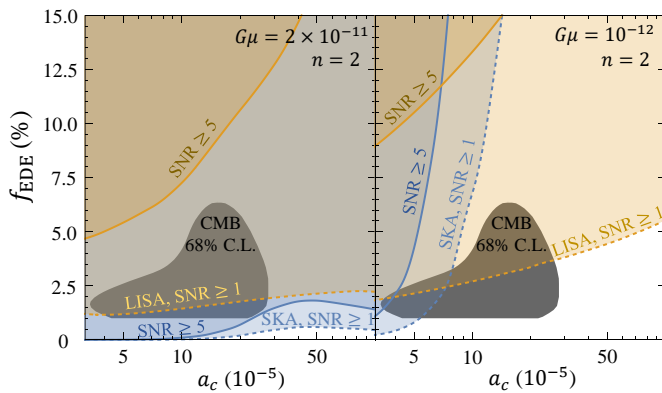


FIG. 4: Energy density fraction of early dark energy  $f_{\text{EDE}}$  versus critical scaling factor  $a_c$  with marking SNR for LISA 4 years operating and SKA 20 years observation period, respectively. The black areas present the CMB analysis with 68% C.L. from [60].

i.e.  $G\mu \geq 2 \times 10^{-11}$  [84, 85], then SKA and LISA should detect EDE signals in future observations. Scanning the  $1\sigma$  regions, detectable EDE signal with  $n = \{2, 3, \infty\}$  requires approximately at least  $G\mu \gtrsim \{4.4, 6.7, 31\} \times 10^{-14}$  and  $G\mu \gtrsim \{4.2, 20, 29\} \times 10^{-13}$  for LISA and SKA, respectively.

### DISTINGUISH SIGNAL FROM OTHER SOURCES

The EDE signal in cosmic string SGWB is distinguishable from other possible influences, such as string parameter variations, or sub-dominated SGWB from astrophysical or cosmological objects. For example, kinks or kink-kink collision modes [91], or string parameters  $\alpha$  and  $\Gamma$  variations [17] would universally influence GW amplitude. Therefore, they cannot cause local amplitude modification as does EDE. We numerically checked that EDE influenced SGWB difference is much flatter than cosmic string SGWB with influence from astrophysical objects, such as binary black hole merger [101, 102] and inspiral [103–105]. On the other hand, a sub-dominated GWs from cosmological phenomena, e.g. flat frequency spectrum from inflation [106–108]; peaky spectrum from domain wall [109, 110]; or first order phase transition dynamics [97, 111, 112]: sound wave [113], bubble wall collision [114, 115] and magnetohydrodynamic turbulence [116, 117], frequency spectra are distinguishable to EDE as well. In particular, the dip structure signal difference at  $f_d$  cannot be caused by any other physical phenomena.

### CONCLUSION

This paper proposed that SGWB originating from cosmic string network can be used to test the Hubble tension solution EDE. EDE behaves as dark energy in the early universe, then begins to dilute at the critical scaling factor  $a_c \sim 10^{-4}$  with total energy density fraction  $f_{\text{EDE}} \gtrsim 1\%$ . It influences cosmic string SGWB by accelerating and decelerating universe expansion rate  $\dot{a}(t)$  due to a dark energy like equation of state  $\omega_\phi = -1$  and diluting faster than or equal to radiation-like component  $\omega_\phi \geq 1/3$ , respectively. The decelerated universe expansion rate locally increases cosmic string GW frequency spectra with magnitude 0.1% to 1% in the frequency range  $10^{-5}$  to  $10^{-3}$  Hz which is within LISA sensitivity. And on the other side, the acceleration reduces spectra with magnitude  $\sim 5\%$  in the lower frequency region  $f \sim 10^{-9}$  Hz, within the SKA search region. We also showed that EDE influenced signals were stronger than LISA and SKA experimental noise background, and hence detectable. Such spectral shapes are distinguishable from other SGWB sourced by cosmological or astrophysical objects. Thus, GW detection provides a possibility to probe EDE.

We considered the simplest EDE effective model [60], but future study will extend to more complex models [61–66] to see whether those can be detected with this method.

### ACKNOWLEDGEMENT

We thank Yanou Cui, Simeon Bird for valuable discussion. CC thanks Ming-Feng Ho for helpful comments on the draft. The author also thanks Academia Sinica for its hospitality. This project is in part supported by the Provost’s Scholars for the Advancement of Physical Sciences fellowship.

### Appendix A: VOS Model

In this appendix, we review the velocity-dependent one-scale (VOS) model that used to predict the string network evolution [118–120], and most of the content can also be found in Refs. [17, 18, 121–123]. The VOS model is used to describe the evolution of long Nambu-Goto string network in terms of a mean string velocity [118–120]

$$\bar{v} = \sqrt{\frac{m}{2} \frac{k(\bar{v})}{[k(\bar{v}) + \bar{c}]}} \left(1 - \frac{2}{m}\right), \quad (11)$$

and a characteristic length,

$$\xi = \frac{m}{2} \sqrt{\frac{k(\bar{v}) [k(\bar{v}) + \bar{c}]}{2(m-2)}}, \quad (12)$$

as a fraction of the horizon, where the  $m$  is exponent of scaling factor in universe energy density  $\rho \propto a^{-m}$ , the chopping parameter  $\bar{c} = 0.23$  [120], and the ansatz function [120]

$$k(\bar{v}) = \frac{2\sqrt{2}}{\pi} (1 - \bar{v}^2) \left( 1 + 2\sqrt{2}\bar{v}^3 \right) \frac{1 - 8\bar{v}^6}{1 + 8\bar{v}^6}. \quad (13)$$

The long string energy density express

$$\rho_L = \frac{\mu}{(\xi t)^2}, \quad (14)$$

and the intercommutation between strings chops them to loops as energy losing as

$$\frac{d\rho_L}{dt} = \bar{c}\bar{v} \frac{\rho_L}{\xi t} = \bar{c}\bar{v} \frac{\mu}{(\xi t)^3}. \quad (15)$$

Consequently, the loops number density at evolution time  $t$  with particular loop size  $\ell(t_i) = \alpha t_i$  that formed at time  $t_i$  reads

$$dn_o(t_i, t) = \frac{0.1}{\alpha} \int_{t_F}^t C_{\text{eff}}(t_i) \frac{dt_i}{t_i^4} \left( \frac{a(t_i)}{a(t)} \right)^3, \quad (16)$$

with

$$C_{\text{eff}}(t_i) = \frac{\bar{c}}{\gamma} \bar{v} \xi^{-3} \quad (17)$$

where  $C_{\text{eff}}$  implies that the energy gain from string network, and  $a^3$  is due to number density dilution. The  $\gamma = \sqrt{2}$  is loop Lorentz boost [92, 93]. EDE locally influences the universe expansion rate around  $a(t) \sim a_c$ , and therefore it would influence the  $C_{\text{eff}}$  on such a period. A smaller  $C_{\text{eff}}$  implies a faster universe expansion rate, i.e. smaller  $m$ . It is because of a less frequently intercommutation rate in a faster expanding universe.

We present  $C_{\text{eff}}$  versus scaling factor  $a$  in Fig. 5, the bumps on the black curve are caused by the changing relativistic degree of freedom in early universe. EDE locally influences  $C_{\text{eff}}$  around  $a_c$  as the colored ranges. Before  $a_c$ , EDE behaves as a cosmological constant that accelerates the universe expansion rate, and therefore  $C_{\text{eff}}$  is smaller than the one in  $\Lambda$ CDM around the  $a_c$ . Shortly after, EDE starts diluting with a dilution rate that is faster or equals to radiation-like components, then the universe expansion rate  $m$  turns to slightly larger than the  $m$  in  $\Lambda$ CDM. Consequently,  $C_{\text{eff}}$  increases to slightly higher than in  $\Lambda$ CDM. All curves converge when EDE energy density isn't comparable to other components.

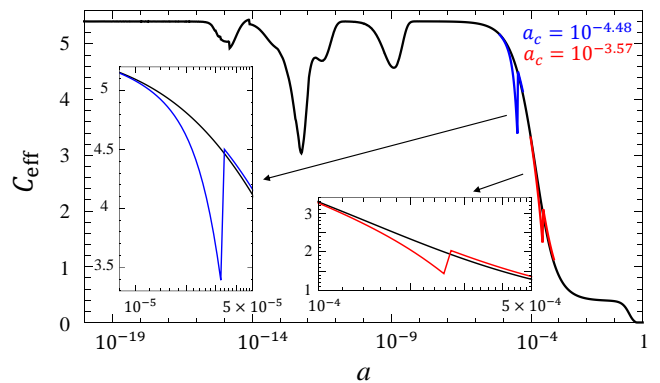


FIG. 5:  $C_{\text{eff}}$  versus scaling factor  $a$ . The black curve is in  $\Lambda$ CDM. The modified universes with the EDE are shown as  $a_c = 10^{-4.48}$  and  $a_c = 10^{-3.57}$  as blue and red, respectively.

## Appendix B: Numerical Details

### Parameters

The cosmological parameters we used in numerical is as following: the scale factor for Hubble expansion rate  $h = 0.71$  [60], pressureless matter density of the universe  $\Omega_m = 0.31$ , dark energy density of the  $\Lambda$ CDM universe  $\Omega_\Lambda = 0.69$ , today temperature  $T_0 = 2.726$  K, and relativistic degrees of freedom  $g_*(T)$  is quoted from [124].

### LISA noise background

To estimate the noise background in the LISA to a stochastic gravitational wave background, we express the result that concluded in [98]. The signal-to-noise ratio is defined as  $\{i = \text{SKA, LISA}\}$

$$\text{SNR} = \sqrt{T_i \int_{f_{\text{min}}}^{f_{\text{max}}} df \left( \frac{\Omega_{\text{GW}}(f)}{\Omega_n^i(f)} \right)^2}, \quad (18)$$

where  $\Omega_{\text{GW}}(f)$  represents the GW signal spectrum,  $T_i$  is experiment operating period, and the integration range is the experiment sensitive region that is  $20 \mu\text{Hz} \leq f \leq 1 \text{Hz}$  in LISA. The effective strain noise spectral spectrum is expressed as

$$\Omega_n^i(f) = S_n^i(f) \frac{2\pi^2 f^3}{3H_0^2}, \quad (19)$$

with the effective noise power spectrum,

$$S_n^{\text{LISA}}(f) \simeq 2\sqrt{2} \frac{20}{3} \left[ \frac{S_I(f)}{(2\pi f)^4} + S_{II} \right] \left[ 1 + \left( \frac{3f}{4f_*} \right)^2 \right] \quad (20)$$

where  $f_* = c/(2\pi L)$  with light speed  $c$  and  $L = 2.5 \times 10^6$  km, and  $S_{II} = 3.6 \times 10^{-41} \text{Hz}^{-1}$  is an optical path-length

fluctuation. The acceleration noise  $S_I(f)$  reads

$$S_I(f) = 5.76 \times 10^{-48} \left[ 1 + \left( \frac{f_1}{f} \right)^2 \right] \text{s}^{-4} \text{Hz}^{-1}, \quad (21)$$

where  $f_1 = 0.4 \text{ mHz}$ . As discussed in [98], the SNR in Eq.(18) is an idealization, we ignore foreground contamination, non-Gaussianity, data interruption, and other systematic issues.

#### SKA noise background

The noise background of interferometer and pulsar timing experiments have been nicely reviewed in the appendix of [97]. As the result, the effective strain noise spectral spectrum is defined as Eq.(19), and the effective noise power spectrum is given [125–127]

$$S_n^{\text{SKA}}(f) = 12\pi^2 f^2 \left[ \frac{2}{N_{\text{SKA}}(N_{\text{SKA}} - 1)} \right]^{1/2} \frac{D_n^{\text{SKA}}}{\zeta_{\text{rms}}}, \quad (22)$$

where  $\zeta_{\text{rms}} \simeq 0.147$ , number of pulsars  $N_{\text{SKA}} = 50$  [90, 128], operating time  $T_{\text{SKA}} = 20 \text{ yrs}$  [97, 129], and the 20 years timing noise spectra  $D_n^{\text{SKA}} \simeq 1.1 \times 10^{-9} \text{ Hz}^{-3}$  [97, 99]. The sensitive frequency range is from the operating period  $f_{\text{min}} = 1/T_{\text{SKA}}$  to the cadence of the timing observation,  $f_{\text{max}} = 1/T_c$  where  $T_c = 1 \text{ week}$  [90, 128].

---

\* Electronic address: [chiafeng.chang@email.ucr.edu](mailto:chiafeng.chang@email.ucr.edu)

- [1] B. P. Abbott *et al.* (LIGO Scientific, Virgo), *Phys. Rev. Lett.* **116**, 061102 (2016), [arXiv:1602.03837 \[gr-qc\]](#).
- [2] B. P. Abbott *et al.* (LIGO Scientific, Virgo), *Phys. Rev. Lett.* **116**, 241103 (2016), [arXiv:1606.04855 \[gr-qc\]](#).
- [3] B. P. Abbott *et al.* (LIGO Scientific, VIRGO), *Phys. Rev. Lett.* **118**, 221101 (2017), [Erratum: *Phys.Rev.Lett.* 121, 129901 (2018)], [arXiv:1706.01812 \[gr-qc\]](#).
- [4] B. P. Abbott *et al.* (LIGO Scientific, Virgo), *Astrophys. J. Lett.* **851**, L35 (2017), [arXiv:1711.05578 \[astro-ph.HE\]](#).
- [5] B. P. Abbott *et al.* (LIGO Scientific, Virgo), *Phys. Rev. Lett.* **119**, 141101 (2017), [arXiv:1709.09660 \[gr-qc\]](#).
- [6] B. P. Abbott *et al.* (LIGO Scientific, Virgo), *Phys. Rev. Lett.* **119**, 161101 (2017), [arXiv:1710.05832 \[gr-qc\]](#).
- [7] B. P. Abbott *et al.* (LIGO Scientific, Virgo, Fermi GBM, INTEGRAL, IceCube, AstroSat Cadmium Zinc Telluride Imager Team, IPN, Insight-Hxmt, ANTARES, Swift, AGILE Team, 1M2H Team, Dark Energy Camera GW-EM, DES, DLT40, GRAWITA, Fermi-LAT, ATCA, ASKAP, Las Cumbres Observatory Group, OzGrav, DWF (Deeper Wider Faster Program), AST3, CAASTRO, VINROUGE, MASTER, J-GEM, GROWTH, JAGWAR, CaltechNRAO, TTU-NRAO, NuSTAR, Pan-STARRS, MAXI Team, TZAC Consortium, KU, Nordic Optical Telescope, ePESSTO, GROND, Texas Tech University, SALT Group, TOROS, BOOTES, MWA, CALET, IKI-GW Follow-up, H.E.S.S., LOFAR, LWA, HAWC, Pierre Auger, ALMA, Euro VLBI Team, Pi of Sky, Chandra Team at McGill University, DFN, ATLAS Telescopes, High Time Resolution Universe Survey, RIMAS, RATIR, SKA South Africa/MeerKAT), *Astrophys. J. Lett.* **848**, L12 (2017), [arXiv:1710.05833 \[astro-ph.HE\]](#).
- [8] L. Lombriser and N. A. Lima, *Phys. Lett. B* **765**, 382 (2017), [arXiv:1602.07670 \[astro-ph.CO\]](#).
- [9] L. Lombriser and A. Taylor, *JCAP* **03**, 031 (2016), [arXiv:1509.08458 \[astro-ph.CO\]](#).
- [10] P. Creminelli and F. Vernizzi, *Phys. Rev. Lett.* **119**, 251302 (2017), [arXiv:1710.05877 \[astro-ph.CO\]](#).
- [11] J. M. Ezquiaga and M. Zumalacárregui, *Phys. Rev. Lett.* **119**, 251304 (2017), [arXiv:1710.05901 \[astro-ph.CO\]](#).
- [12] T. Baker, E. Bellini, P. G. Ferreira, M. Lagos, J. Noller, and I. Sawicki, *Phys. Rev. Lett.* **119**, 251301 (2017), [arXiv:1710.06394 \[astro-ph.CO\]](#).
- [13] J. Sakstein and B. Jain, *Phys. Rev. Lett.* **119**, 251303 (2017), [arXiv:1710.05893 \[astro-ph.CO\]](#).
- [14] C.-F. Chang and Y. Cui, (2021), [arXiv:2106.09746 \[hep-ph\]](#).
- [15] C.-F. Chang and Y. Cui, *Phys. Dark Univ.* **29**, 100604 (2020), [arXiv:1910.04781 \[hep-ph\]](#).
- [16] R. R. Caldwell, T. L. Smith, and D. G. E. Walker, *Phys. Rev. D* **100**, 043513 (2019), [arXiv:1812.07577 \[astro-ph.CO\]](#).
- [17] Y. Cui, M. Lewicki, D. E. Morrissey, and J. D. Wells, *JHEP* **01**, 081 (2019), [arXiv:1808.08968 \[hep-ph\]](#).
- [18] Y. Cui, M. Lewicki, D. E. Morrissey, and J. D. Wells, *Phys. Rev. D* **97**, 123505 (2018), [arXiv:1711.03104 \[hep-ph\]](#).
- [19] R. A. Battye and E. P. S. Shellard, *Phys. Rev. Lett.* **73**, 2954 (1994), [Erratum: *Phys.Rev.Lett.* 76, 2203–2204 (1996)], [arXiv:astro-ph/9403018](#).
- [20] S. Blasi, V. Brdar, and K. Schmitz, *Phys. Rev. Res.* **2**, 043321 (2020), [arXiv:2004.02889 \[hep-ph\]](#).
- [21] Y. Gouttenoire, G. Servant, and P. Simakachorn, *JCAP* **07**, 016 (2020), [arXiv:1912.03245 \[hep-ph\]](#).
- [22] B. P. Abbott *et al.* (LIGO Scientific, Virgo, 1M2H, Dark Energy Camera GW-E, DES, DLT40, Las Cumbres Observatory, VINROUGE, MASTER), *Nature* **551**, 85 (2017), [arXiv:1710.05835 \[astro-ph.CO\]](#).
- [23] S. Mukherjee, G. Lavaux, F. R. Bouchet, J. Jasche, B. D. Wandelt, S. M. Nissanke, F. Leclercq, and K. Hotokezaka, *Astron. Astrophys.* **646**, A65 (2021), [arXiv:1909.08627 \[astro-ph.CO\]](#).
- [24] V. Gayathri, J. Healy, J. Lange, B. O’Brien, M. Szczepanczyk, I. Bartos, M. Campanelli, S. Klimenko, C. Lousto, and R. O’Shaughnessy, (2020), [arXiv:2009.14247 \[astro-ph.HE\]](#).
- [25] S. Mukherjee, A. Ghosh, M. J. Graham, C. Karathanasis, M. M. Kasliwal, I. Magaña Hernandez, S. M. Nissanke, A. Silvestri, and B. D. Wandelt, (2020), [arXiv:2009.14199 \[astro-ph.CO\]](#).
- [26] A. G. Riess *et al.*, *Astrophys. J.* **826**, 56 (2016), [arXiv:1604.01424 \[astro-ph.CO\]](#).
- [27] A. G. Riess *et al.*, *Astrophys. J.* **861**, 126 (2018), [arXiv:1804.10655 \[astro-ph.CO\]](#).
- [28] L. Breuval *et al.*, *Astron. Astrophys.* **643**, A115 (2020), [arXiv:2006.08763 \[astro-ph.SR\]](#).
- [29] A. G. Riess, S. Casertano, W. Yuan, J. B. Bowers,

- L. Macri, J. C. Zinn, and D. Scolnic, *Astrophys. J. Lett.* **908**, L6 (2021), arXiv:2012.08534 [astro-ph.CO] .
- [30] J. Soltis, S. Casertano, and A. G. Riess, *Astrophys. J. Lett.* **908**, L5 (2021), arXiv:2012.09196 [astro-ph.GA] .
- [31] W. L. Freedman, B. F. Madore, T. Hoyt, I. S. Jang, R. Beaton, M. G. Lee, A. Monson, J. Neelley, and J. Rich, (2020), 10.3847/1538-4357/ab7339, arXiv:2002.01550 [astro-ph.GA] .
- [32] V. Bonvin *et al.*, *Mon. Not. Roy. Astron. Soc.* **465**, 4914 (2017), arXiv:1607.01790 [astro-ph.CO] .
- [33] S. Birrer *et al.*, *Mon. Not. Roy. Astron. Soc.* **484**, 4726 (2019), arXiv:1809.01274 [astro-ph.CO] .
- [34] P. Denzel, J. P. Coles, P. Saha, and L. L. R. Williams, *Mon. Not. Roy. Astron. Soc.* **501**, 784 (2021), arXiv:2007.14398 [astro-ph.CO] .
- [35] T. Yang, S. Birrer, and B. Hu, *Mon. Not. Roy. Astron. Soc.* **497**, L56 (2020), arXiv:2003.03277 [astro-ph.CO] .
- [36] S. Birrer *et al.*, *Astron. Astrophys.* **643**, A165 (2020), arXiv:2007.02941 [astro-ph.CO] .
- [37] M. Millon *et al.*, *Astron. Astrophys.* **639**, A101 (2020), arXiv:1912.08027 [astro-ph.CO] .
- [38] E. J. Baxter and B. D. Sherwin, *Mon. Not. Roy. Astron. Soc.* **501**, 1823 (2021), arXiv:2007.04007 [astro-ph.CO] .
- [39] N. Aghanim *et al.* (Planck), *Astron. Astrophys.* **641**, A6 (2020), arXiv:1807.06209 [astro-ph.CO] .
- [40] K. Aylor *et al.* (SPT), *Astrophys. J.* **850**, 101 (2017), arXiv:1706.10286 [astro-ph.CO] .
- [41] S. Aiola *et al.* (ACT), *JCAP* **12**, 047 (2020), arXiv:2007.07288 [astro-ph.CO] .
- [42] S. K. Choi *et al.* (ACT), *JCAP* **12**, 045 (2020), arXiv:2007.07289 [astro-ph.CO] .
- [43] S. M. Feeney, D. J. Mortlock, and N. Dalmaso, *Mon. Not. Roy. Astron. Soc.* **476**, 3861 (2018), arXiv:1707.00007 [astro-ph.CO] .
- [44] B. R. Zhang, M. J. Childress, T. M. Davis, N. V. Karpenka, C. Lidman, B. P. Schmidt, and M. Smith, *Mon. Not. Roy. Astron. Soc.* **471**, 2254 (2017), arXiv:1706.07573 [astro-ph.CO] .
- [45] W. Cardona, M. Kunz, and V. Pettorino, *JCAP* **03**, 056 (2017), arXiv:1611.06088 [astro-ph.CO] .
- [46] C. L. Bennett, D. Larson, J. L. Weiland, and G. Hinshaw, *Astrophys. J.* **794**, 135 (2014), arXiv:1406.1718 [astro-ph.CO] .
- [47] D. W. Pesce *et al.*, *Astrophys. J. Lett.* **891**, L1 (2020), arXiv:2001.09213 [astro-ph.CO] .
- [48] K. C. Wong *et al.*, *Mon. Not. Roy. Astron. Soc.* **498**, 1420 (2020), arXiv:1907.04869 [astro-ph.CO] .
- [49] C. D. Huang, A. G. Riess, W. Yuan, L. M. Macri, N. L. Zakamska, S. Casertano, P. A. Whitelock, S. L. Hoffmann, A. V. Filippenko, and D. Scolnic, (2019), 10.3847/1538-4357/ab5dbd, arXiv:1908.10883 [astro-ph.CO] .
- [50] W. L. Freedman *et al.*, (2019), 10.3847/1538-4357/ab2f73, arXiv:1907.05922 [astro-ph.CO] .
- [51] G. F. Benedict, B. E. McArthur, M. W. Feast, T. G. Barnes, T. E. Harrison, R. J. Patterson, J. W. Menzies, J. L. Bean, and W. L. Freedman, *Astron. J.* **133**, 1810 (2007), [Erratum: *Astron. J.* 133, 2980 (2007)], arXiv:astro-ph/0612465 .
- [52] E. M. L. Humphreys, M. J. Reid, J. M. Moran, L. J. Greenhill, and A. L. Argon, *Astrophys. J.* **775**, 13 (2013), arXiv:1307.6031 [astro-ph.CO] .
- [53] G. Efstathiou, *Mon. Not. Roy. Astron. Soc.* **440**, 1138 (2014), arXiv:1311.3461 [astro-ph.CO] .
- [54] M. Rigault *et al.*, *Astrophys. J.* **802**, 20 (2015), arXiv:1412.6501 [astro-ph.CO] .
- [55] W. D. Kenworthy, D. Scolnic, and A. Riess, *Astrophys. J.* **875**, 145 (2019), arXiv:1901.08681 [astro-ph.CO] .
- [56] D. N. Spergel, R. Flauger, and R. Hložek, *Phys. Rev. D* **91**, 023518 (2015), arXiv:1312.3313 [astro-ph.CO] .
- [57] L. Knox and M. Millea, *Phys. Rev. D* **101**, 043533 (2020), arXiv:1908.03663 [astro-ph.CO] .
- [58] L. Verde, T. Treu, and A. G. Riess, *Nature Astron.* **3**, 891 (2019), arXiv:1907.10625 [astro-ph.CO] .
- [59] K. Aylor, M. Joy, L. Knox, M. Millea, S. Raghunathan, and W. L. K. Wu, *Astrophys. J.* **874**, 4 (2019), arXiv:1811.00537 [astro-ph.CO] .
- [60] V. Poulin, T. L. Smith, T. Karwal, and M. Kamionkowski, *Phys. Rev. Lett.* **122**, 221301 (2019), arXiv:1811.04083 [astro-ph.CO] .
- [61] V. Poulin, T. L. Smith, D. Grin, T. Karwal, and M. Kamionkowski, *Phys. Rev. D* **98**, 083525 (2018), arXiv:1806.10608 [astro-ph.CO] .
- [62] T. L. Smith, V. Poulin, and M. A. Amin, *Phys. Rev. D* **101**, 063523 (2020), arXiv:1908.06995 [astro-ph.CO] .
- [63] P. Agrawal, F.-Y. Cyr-Racine, D. Pinner, and L. Randall, (2019), arXiv:1904.01016 [astro-ph.CO] .
- [64] T. L. Smith, V. Poulin, J. L. Bernal, K. K. Boddy, M. Kamionkowski, and R. Murgia, (2020), arXiv:2009.10740 [astro-ph.CO] .
- [65] R. Murgia, G. F. Abellán, and V. Poulin, *Phys. Rev. D* **103**, 063502 (2021), arXiv:2009.10733 [astro-ph.CO] .
- [66] M.-X. Lin, W. Hu, and M. Raveri, *Phys. Rev. D* **102**, 123523 (2020), arXiv:2009.08974 [astro-ph.CO] .
- [67] E. J. Copeland, M. Sami, and S. Tsujikawa, *Int. J. Mod. Phys. D* **15**, 1753 (2006), arXiv:hep-th/0603057 .
- [68] E. V. Linder, *Gen. Rel. Grav.* **40**, 329 (2008), arXiv:0704.2064 [astro-ph] .
- [69] C.-F. Chang and Y. Cui, *Phys. Rev. D* **102**, 015003 (2020), arXiv:1911.11885 [hep-ph] .
- [70] A. Vilenkin, *Phys. Rept.* **121**, 263 (1985).
- [71] R. R. Caldwell and B. Allen, *Phys. Rev. D* **45**, 3447 (1992).
- [72] M. B. Hindmarsh and T. W. B. Kibble, *Rept. Prog. Phys.* **58**, 477 (1995), arXiv:hep-ph/9411342 .
- [73] T. W. B. Kibble, *J. Phys.* **A9**, 1387 (1976).
- [74] H. B. Nielsen and P. Olesen, *Nucl. Phys.* **B61**, 45 (1973).
- [75] T. Vachaspati and A. Vilenkin, *Phys. Rev. D* **30**, 2036 (1984).
- [76] A. Vilenkin and E. P. S. Shellard, *Cosmic Strings and Other Topological Defects* (Cambridge University Press, 2000).
- [77] E. J. Copeland, R. C. Myers, and J. Polchinski, *JHEP* **06**, 013 (2004), arXiv:hep-th/0312067 .
- [78] G. Dvali and A. Vilenkin, *JCAP* **03**, 010 (2004), arXiv:hep-th/0312007 .
- [79] J. Polchinski, in *NATO Advanced Study Institute and EC Summer School on String Theory: From Gauge Interactions to Cosmology* (2004) arXiv:hep-th/0412244 .
- [80] M. G. Jackson, N. T. Jones, and J. Polchinski, *JHEP* **10**, 013 (2005), arXiv:hep-th/0405229 .
- [81] L. Lentati *et al.*, *Mon. Not. Roy. Astron. Soc.* **453**, 2576 (2015), arXiv:1504.03692 [astro-ph.CO] .
- [82] R. M. Shannon *et al.*, *Science* **349**, 1522 (2015), arXiv:1509.07320 [astro-ph.CO] .
- [83] Z. Arzoumanian *et al.* (NANOGrav), *Astrophys. J. Lett.*

- 905**, L34 (2020), arXiv:2009.04496 [astro-ph.HE] .
- [84] J. Ellis and M. Lewicki, *Phys. Rev. Lett.* **126**, 041304 (2021), arXiv:2009.06555 [astro-ph.CO] .
- [85] S. Blasi, V. Brdar, and K. Schmitz, *Phys. Rev. Lett.* **126**, 041305 (2021), arXiv:2009.06607 [astro-ph.CO] .
- [86] J. S. Hazboun, J. Simon, X. Siemens, and J. D. Romano, *Astrophys. J. Lett.* **905**, L6 (2020), arXiv:2009.05143 [astro-ph.IM] .
- [87] P. Amaro-Seoane *et al.* (LISA), (2017), arXiv:1702.00786 [astro-ph.IM] .
- [88] N. Bartolo *et al.*, *JCAP* **12**, 026 (2016), arXiv:1610.06481 [astro-ph.CO] .
- [89] C. Caprini, D. G. Figueroa, R. Flauger, G. Nardini, M. Peloso, M. Pieroni, A. Ricciardone, and G. Tasinato, *JCAP* **11**, 017 (2019), arXiv:1906.09244 [astro-ph.CO] .
- [90] G. Janssen *et al.*, *PoS AASKA14*, 037 (2015), arXiv:1501.00127 [astro-ph.IM] .
- [91] P. Auclair *et al.*, *JCAP* **04**, 034 (2020), arXiv:1909.00819 [astro-ph.CO] .
- [92] J. J. Blanco-Pillado, K. D. Olum, and B. Shlaer, *Phys. Rev. D* **89**, 023512 (2014), arXiv:1309.6637 [astro-ph.CO] .
- [93] J. J. Blanco-Pillado and K. D. Olum, *Phys. Rev. D* **96**, 104046 (2017), arXiv:1709.02693 [astro-ph.CO] .
- [94] A. Vilenkin, *Phys. Lett. B* **107**, 47 (1981).
- [95] N. Turok, *Nucl. Phys. B* **242**, 520 (1984).
- [96] J. M. Quashnock and D. N. Spergel, *Phys. Rev. D* **42**, 2505 (1990).
- [97] K. Schmitz, *JHEP* **01**, 097 (2021), arXiv:2002.04615 [hep-ph] .
- [98] T. L. Smith and R. Caldwell, *Phys. Rev. D* **100**, 104055 (2019), arXiv:1908.00546 [astro-ph.CO] .
- [99] E. Thrane and J. D. Romano, *Phys. Rev. D* **88**, 124032 (2013), arXiv:1310.5300 [astro-ph.IM] .
- [100] J. D. Romano and N. J. Cornish, *Living Rev. Rel.* **20**, 2 (2017), arXiv:1608.06889 [gr-qc] .
- [101] I. Cholis, *JCAP* **06**, 037 (2017), arXiv:1609.03565 [astro-ph.HE] .
- [102] V. Mandic, S. Bird, and I. Cholis, *Phys. Rev. Lett.* **117**, 201102 (2016), arXiv:1608.06699 [astro-ph.CO] .
- [103] M. Bonetti and A. Sesana, *Phys. Rev. D* **102**, 103023 (2020), arXiv:2007.14403 [astro-ph.GA] .
- [104] S. Babak, J. Gair, A. Sesana, E. Barausse, C. F. Sopuerta, C. P. L. Berry, E. Berti, P. Amaro-Seoane, A. Petiteau, and A. Klein, *Phys. Rev. D* **95**, 103012 (2017), arXiv:1703.09722 [gr-qc] .
- [105] P. Amaro-Seoane, J. R. Gair, M. Freitag, M. Coleman Miller, I. Mandel, C. J. Cutler, and S. Babak, *Class. Quant. Grav.* **24**, R113 (2007), arXiv:astro-ph/0703495 .
- [106] M. S. Turner, M. J. White, and J. E. Lidsey, *Phys. Rev. D* **48**, 4613 (1993), arXiv:astro-ph/9306029 .
- [107] L. A. Boyle and P. J. Steinhardt, *Phys. Rev. D* **77**, 063504 (2008), arXiv:astro-ph/0512014 .
- [108] C. Caprini and D. G. Figueroa, *Class. Quant. Grav.* **35**, 163001 (2018), arXiv:1801.04268 [astro-ph.CO] .
- [109] K. Saikawa, *Universe* **3**, 40 (2017), arXiv:1703.02576 [hep-ph] .
- [110] T. Hiramatsu, M. Kawasaki, and K. Saikawa, *JCAP* **02**, 031 (2014), arXiv:1309.5001 [astro-ph.CO] .
- [111] C. Caprini, R. Durrer, T. Konstandin, and G. Servant, *Phys. Rev. D* **79**, 083519 (2009), arXiv:0901.1661 [astro-ph.CO] .
- [112] T. Alanne, T. Hügler, M. Platscher, and K. Schmitz, *JHEP* **03**, 004 (2020), arXiv:1909.11356 [hep-ph] .
- [113] M. Hindmarsh, S. J. Huber, K. Rummukainen, and D. J. Weir, *Phys. Rev. D* **92**, 123009 (2015), arXiv:1504.03291 [astro-ph.CO] .
- [114] S. J. Huber and T. Konstandin, *JCAP* **09**, 022 (2008), arXiv:0806.1828 [hep-ph] .
- [115] D. J. Weir, *Phys. Rev. D* **93**, 124037 (2016), arXiv:1604.08429 [astro-ph.CO] .
- [116] C. Caprini, R. Durrer, and G. Servant, *JCAP* **12**, 024 (2009), arXiv:0909.0622 [astro-ph.CO] .
- [117] P. Binetruy, A. Bohe, C. Caprini, and J.-F. Dufaux, *JCAP* **06**, 027 (2012), arXiv:1201.0983 [gr-qc] .
- [118] C. J. A. P. Martins and E. P. S. Shellard, *Phys. Rev. D* **53**, 575 (1996), arXiv:hep-ph/9507335 .
- [119] C. J. A. P. Martins and E. P. S. Shellard, *Phys. Rev. D* **54**, 2535 (1996), arXiv:hep-ph/9602271 .
- [120] C. J. A. P. Martins and E. P. S. Shellard, *Phys. Rev. D* **65**, 043514 (2002), arXiv:hep-ph/0003298 .
- [121] P. P. Avelino and L. Sousa, *Phys. Rev. D* **85**, 083525 (2012), arXiv:1202.6298 [astro-ph.CO] .
- [122] L. Sousa and P. P. Avelino, *Phys. Rev. D* **88**, 023516 (2013), arXiv:1304.2445 [astro-ph.CO] .
- [123] Y. Gouttenoire, G. Servant, and P. Simakachorn, *JCAP* **07**, 032 (2020), arXiv:1912.02569 [hep-ph] .
- [124] K. Saikawa and S. Shirai, *JCAP* **05**, 035 (2018), arXiv:1803.01038 [hep-ph] .
- [125] C. J. Moore, S. R. Taylor, and J. R. Gair, *Class. Quant. Grav.* **32**, 055004 (2015), arXiv:1406.5199 [astro-ph.IM] .
- [126] J. S. Hazboun, J. D. Romano, and T. L. Smith, *Phys. Rev. D* **100**, 104028 (2019), arXiv:1907.04341 [gr-qc] .
- [127] R. w. Hellings and G. s. Downs, *Astrophys. J. Lett.* **265**, L39 (1983).
- [128] C. J. Moore, R. H. Cole, and C. P. L. Berry, *Class. Quant. Grav.* **32**, 015014 (2015), arXiv:1408.0740 [gr-qc] .
- [129] X. Siemens, J. Ellis, F. Jenet, and J. D. Romano, *Class. Quant. Grav.* **30**, 224015 (2013), arXiv:1305.3196 [astro-ph.IM] .